ELSEVIER

Polymer 41 (2000) 6301–6310

polymer

Molecular dependence of the essential and non-essential work of fracture of amorphous films of poly(ethylene-2,6-naphthalate) (PEN)

J. Karger-Kocsis[a,*], E.J. Moskala[b]

[a]*Institut für Verbundwerkstoffe GmbH, Universität Kaiserslautern, Erwin-Schrödinger-Strasse, P.O. Box 3049, D-67653 Kaiserslautern, Germany*
[b]*Eastman Chemical Co., Research Laboratories, P.O. Box 1972, Kingsport, TN 37662-5150, USA*

Received 12 July 1999; received in revised form 8 November 1999; accepted 22 November 1999

Abstract

Plane stress fracture toughness of amorphous films of poly(ethylene-2,6-naphthalate) (PEN) with various molecular weights (MW; characterized by the intrinsic viscosity, IV) was determined by the essential work of fracture (EWF) concept using tensile-loaded deeply double-edge notched (DDEN-T) specimens. These PENs met the basic requirement of the EWF concept: full ligament yielding, which was marked by a load drop in the force–displacement curves of the DDEN-T specimens, preceded the crack growth. This "load mark" allowed us to partition between yielding and necking. The yielding-related EWF terms were not affected by the MW of the resins and thus served for the comparison of the results. It is argued that the EWF response is governed by the entanglement network density. The role of entanglements was substantiated by showing that the "plastic" zone developed via cold drawing and not by true plastic deformation. On the other hand, MW influenced the necking related EWF terms. High MW PENs failed by stable crack growth, whereas low MW resins experienced unstable crack growth (more exactly a transition from stable to unstable crack growth) in the necking phase. This was traced to the load distribution capacity of the long entangled chains. Attempts were also made to estimate the essential and non-essential work of fracture parameters and their constituents from uniaxial tensile tests performed on dumbbells.

Keywords: Essential work of fracture; Poly(ethylene naphthalate); Molecular weight

1. Introduction

The essential work of fracture (EWF) theory, credited to Broberg [1,2] and recently reviewed by Mai et al. [3] is a suitable technique to assess the toughness of ductile polymers, and especially films in which plane stress conditions prevail [4–7]. The EWF concept constitutes a difference between the essential work required to fracture the polymer in its process zone (W_e) and the non-essential or plastic work consumed by various deformation mechanisms in the plastic zone (W_p). The total work of fracture (W_f) is composed of the two above terms:

$$W_f = W_e + W_p \tag{1}$$

Taking into consideration that W_e is surface-related, whereas W_p is volume-related, W_f can be given by the related specific work terms (i.e. w_e and w_p, respectively):

$$W_f = w_e lt + \beta w_p l^2 t \tag{2}$$

$$w_f = \frac{W_f}{lt} = w_e + \beta w_p l \tag{3}$$

where l is the ligament length, t the thickness of the specimen and β a shape factor related to the form of the plastic zone. Based on Eq. (3) the specific essential work of fracture (w_e) can be easily determined by reading the ordinate intercept of the linear plot w_f vs l. It was recently shown that the amorphous copolyesters are likely the best model substances when adopting the EWF method [7–9]. This was argued by the easy yielding (which occurs via shear banding and shear yielding [7,10]) of amorphous copolyesters where the specimen ligament is fully yielded prior to crack growth [7–9,11]. Note that this behavior is still very seldom observed in the present EWF literature [6,12]. On the contrary, this is a must if the morphological or molecular dependence of the EWF parameters is targeted. This behavior allows us to make a clear distinction between the effects of the initial (preyielding) and loading-induced structural changes (postyielding).

The molecular and morphological dependence of the fracture mechanical parameters is currently of great interest [13,14]. Some preliminary results, achieved on amorphous copolyesters, suggest that it is not the molecular weight

* Corresponding author. Fax: +49-6312017198.
E-mail address: karger@ivw.uni-kl.de (J. Karger-Kocsis).

0032-3861/00/$ - see front matter
PII: S0032-3861(99)00866-6

Table 1
Basic molecular and mechanical characteristics of the amorphous PEN films studied. Note: the mechanical parameters are mean values of five parallel tests

Material	Thickness (mm)	IV (dl/g)	E (GPa)	σ_y (MPa)	ϵ_y (%)	σ_n (MPa)	ϵ_b (%)
PEN-1	≈ 0.2	0.588	2.10	66.8	6.9	50	<10
PEN-2	≈ 0.5	0.690	2.02	64.2	7.0	50	<50
PEN-3	≈ 0.5	0.899	1.93	62.0	8.0	47	>100
PEN-4	≈ 0.5	0.963	1.90	61.0	9.0	46	>100

(MW), but the MW between the entanglements (M_e) or entanglement density that governs the yielding-related specific essential work of fracture ($w_{e,y}$) [9,11]. The latter parameter was believed to agree with the plane strain value $w_{e,I}$, where I stands for mode I type crack tip opening [8]. The dependence of fracture-related mechanical parameters on molecular entanglements is in concert with some predictions deduced for amorphous glassy polymers undergoing crazing during fracture [15,16]. Apart from the entanglement density, the MW of the polymer is also believed to be a critical parameter [17].

The objective of this work is to determine the EWF parameters of films of amorphous poly(ethylene-2,6-naphthalate) (PEN). This material was selected because it shows full ligament yielding prior to crack growth and thus meets the aforementioned application requirements of the EWF, and its fracture behavior is very sensitive to changes in the MW. The main aim of this study was to establish which EWF parameters, if any, depend on the entanglement network and MW characteristics.

2. Experimental

2.1. Materials

Films with a thickness of ca. 0.5 mm (except of PEN-1 of ca. 0.2 mm) were produced from homopolymer grades of PEN with varying MW and supplied by the Eastman Chemical Company, Kingsport, TN, USA. The inherent viscosity (IV) of the PENs was determined at 25°C using solutions containing 0.5 g of polymer per 100 ml of a 60/40 pentafluorophenol/trichlorobenzene mixture. IV ranged from 0.588 to 0.963 dl/g (see Table 1).

2.2. Tests

2.2.1. Material characterization

The thermal response of the PEN films was studied by differential scanning calorimetry (DSC) and dynamic-mechanical thermal analysis (DMTA). DSC traces were recorded on a Mettler DSC 30 at heating and cooling rates of 10°C/min. DMTA spectra were taken in tensile mode on an Eplexor 150 N Qualimeter (Gabo) using a frequency of 10 Hz and a heating rate of 5°C/min. The static and oscillating loads were set for 5 and ± 2 N, respectively. DMTA tests were terminated at ca. 260°C when the specimen, which crystallized from the melt during the test, failed by thermal fracture.

2.2.2. Mechanical testing

The mechanical tests reported here were performed at room temperature (RT) on a Zwick 1445 universal testing machine using a crosshead speed of 1 mm/min. Tensile-modulus (E), yield strength (σ_y), elongation at yield (ϵ_y), necking strength (σ_n) and elongation at break (ϵ_b) were determined (cf. Table 1) by using dumbbell specimens (No. 3 according to DIN 53 455). The same dumbbell specimen was used to determine the specific plastic work (w_p).

For the EWF study, double deeply edge-notched tensile (DDEN-T) specimens with a width of 35 mm and overall length of 100 mm (clamped length 70 mm) were selected. The free ligament length (l) ranged from $l = 5$ to 20 mm. At every ligament length, at least three specimens were investigated. Data reduction (cf.Eq. (3)) followed the recommendations of the ESIS TC-4 group [18]. The specific work of fracture (w_f) and its yielding-related ($w_{f,y}$) and necking-related ($w_{f,n}$) parts were determined as described in our previous works [9,11]— see also Section 3.3.

The non-essential or plastic work (w_p) was derived by two methods: from tensile tests on dumbbells, and by assessing the shape of the plastic zone using light microscopy and infrared thermography (IRT, Hughes Thermovision, Portland, OR) [11]. For the uniaxial tensile tests w_p is given directly by the ratio of the total fracture energy (calculated from the area beneath the load–displacement curve) to the necked volume of the dumbbell specimen. In the case of light microscopy and IRT the shape parameter (β) was derived by inspecting the final plastic zone post-mortem (light microscopy) or its development in situ (IRT). Viewing of the plastic zone by light microscopy occurred on failed DDEN-T specimens. In contrast, IRT was videotaped continuously during loading. Since IRT was aimed at mapping the relative temperature rise in the ligament region an arbitrarily chosen emission factor ($= 0.9$) was chosen. For the direct and indirect determinations of the plastic work the interested reader is referred to our previous works [7–9,11].

3. Results and discussion

3.1. Thermal and thermomechanical behavior

In the DSC traces in Fig. 1, the glass transition step at ca. 118°C, the cold crystallization peak ranging from 190 to 220°C, and the subsequent melting peak at ca. 260°C are well resolved. Comparing the DSC traces of PENs of low

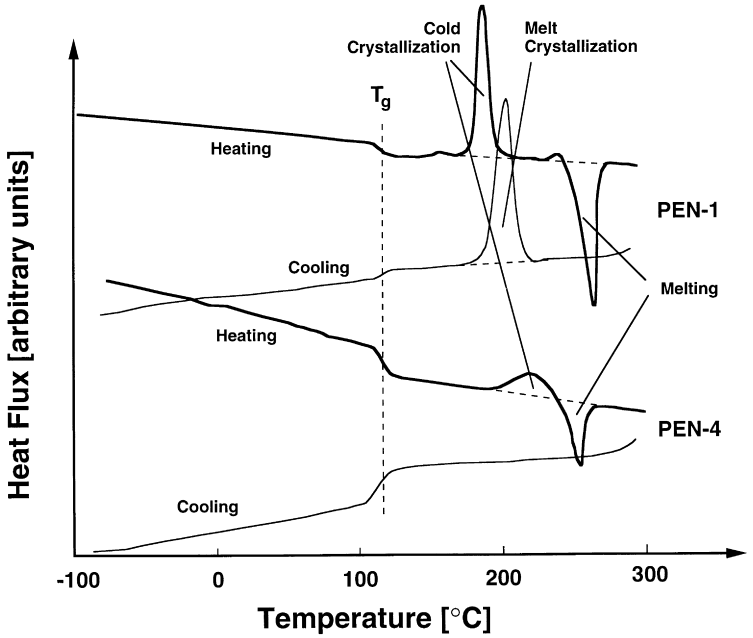

Fig. 1. DSC heating and cooling traces for PEN-1 and PEN-4.

(no. 1) and high IV (no. 4), one can recognize that low IV (and thus low MW) favors both the cold crystallization and the crystallization from the melt. For PEN of high IV the cold crystallization shifted toward higher temperatures, and in addition, no melt crystallization could be observed during cooling (cf. Fig. 1). In the DMTA traces showing the complex *E*-modulus (E^*) and mechanical loss factor (tan δ) as a function of temperature (T) the T_g (stiffness drop at ca. 110°C) and cold crystallization (stiffness increase reaching a maximum at ca. 185°C) are well reflected (cf. Fig. 2). The reason why the cold crystallization during the DMTA test started earlier than in case of the DSC is due to the applied tensile loading. Tensile loading contributes to strain-induced crystallization in amorphous copolyesters [19]. In the tan δ vs T trace three relaxation peaks appeared: the T_g, a shoulder at ca. 75°C and a further secondary relaxation at ca. −70°C. The shoulder can be assigned to the relative motion of the naphthalene rings, whereas the peak

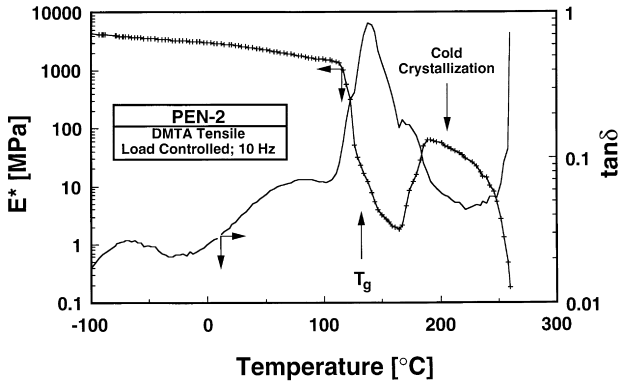

Fig. 2. DMTA spectrum (E^* and tan δ vs T) of PEN-2 polymer.

at −70°C to those of the carboxyl side groups according to Cañadas et al. [20].

3.2. Validation of the EWF approach

Fig. 3 depicts the load–displacement (F–x) curves of DDENT-T specimens at various ligaments for a PEN of high IV (no. 3). It is very striking that the F–x curves at different ligament length are similar to one another, so that one of the basic requirement of the EWF theory is met. A more important phenomenon with respect to the F–x curves is related to a load drop, indicated by arrows in these traces, that identifies where the yielding terminates and the onset of necking takes place. At this point the entire ligament yields instantaneously as shown by the related IRT frames (see Fig. 4 picture B). The ligament yielding was followed by the formation of the plastic zone (cf. Fig. 4, picture C). According to the IRT frames, the temperature rises by 4–5°C due to the sudden yielding. The serial IRT pictures in Fig. 4 mirror the temperature field in the ligament area. The cursor points 1–5 on the IRT frames were positioned to show the reference temperature (1), the temperature at both notch regions (2 and 3), and that of the plastic and process zones (4 and 5), respectively. The IRT frames before final separation of the specimens hint for the development a shallow, diamond-like plastic zone. This agreed with the light microscopic observation (see Section 3.5). This behavior resembles that of poly(ethylene terephthalate) and related amorphous copolyesters [7–9,11].

The above scenario changed substantially for a PEN of low MW (i.e. low IV). First, the F–x curves are no longer similar to each other. Differences are apparent in the post-yielding, necking stage, although yielding seems to preserve

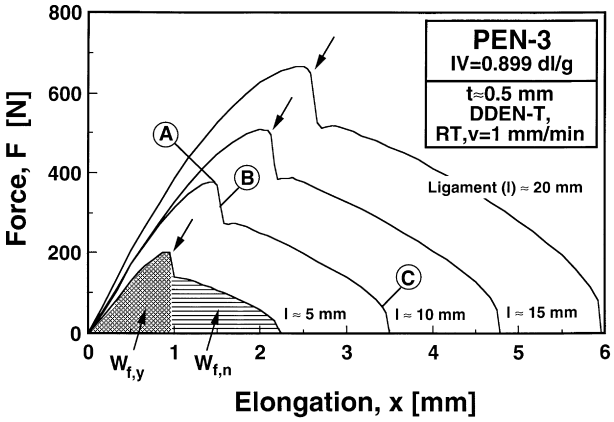

Fig. 3. Comparison of the F–x curves of DDEN-T specimens at different ligament lengths ($l \approx 5$, ≈ 10, ≈ 15 and ≈ 20 mm) for PEN-3 Note:this figure also indicates the partition between yielding and necking.

the self-similarity (cf. Fig. 5). The difference in the necking stage is attributed to crack instability, which occurred in the low MW PEN. The fact that full ligament yielding still precedes the necking accompanied with unstable crack growth is well reflected by the related IRT frames in Fig. 6. Accordingly, the crack tips blunt initially (Fig. 6A). This is followed by the full ligament yielding (Fig. 6B) marked by the load drop (cf. related F–x curve in Fig. 5). Afterwards, the DDEN-T specimen broke in a brittle manner with little or without necking—cf. Fig. 6C.

For the validity of the EWF approach the ligament range and specimen-related constraint effects should be considered. The usual size criteria of the EWF tests are as follows [3,18 and references therein]:

$$(3-5)t \le l \le \left(\frac{B}{3} \text{ or } 2r_p\right) \tag{4}$$

where B is the width of the specimen (35 mm) and $2r_p$ is the size of the plastic zone:

$$2r_p = \frac{1}{\pi}\frac{Ew_e}{\sigma_y^2} \tag{5}$$

The ligament of our test specimens were always beyond the lower threshold (ca. 1.5 mm in this case). On the contrary, it was claimed in several works that the upper threshold criteria are much too conservative [8,9]. The plastic zone calculated by inserting the following mechanical data: $E = 2.0$ GPa, $w_e = 45$ kJ/m^2 and $\sigma_y = 60$ MPa (see in Tables 1 and 2), yielded $2r_p \approx 8$ mm. This size is even smaller than the alternative width criterion ($B/3 \approx 12$ mm). Both of them are, however, far below that actual ligament where still the self-similarity of the F–x curves could be observed (ca. 20 mm). Note that the above values are related to PENs of high MW. The criterion in Eq. (5) can hardly be adopted for the PENs of low MW as their w_e values are strongly affected by the scatter caused by crack instability in the necking phase (see Section 3.4). Therefore, the net section

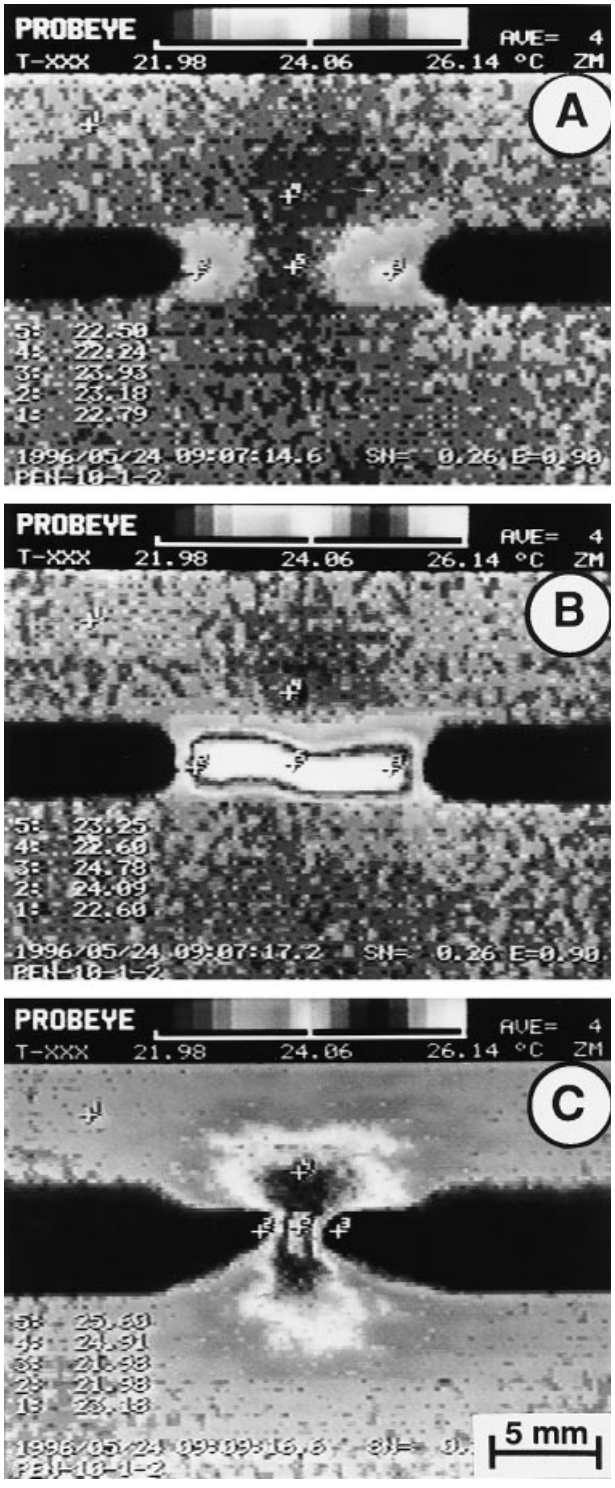

Fig. 4. Serial IRT frames taken during loading of a DDEN-T specimen of $l \approx 10$ mm of PEN-3 Note: the taking position of the IRT frames are shown in the related F–x curve in Fig. 3.

stress (σ_N):

$$\sigma_N = \frac{F_{max}}{lt} \tag{6}$$

where F_{max} is the maximum load during testing of the DDEN-T

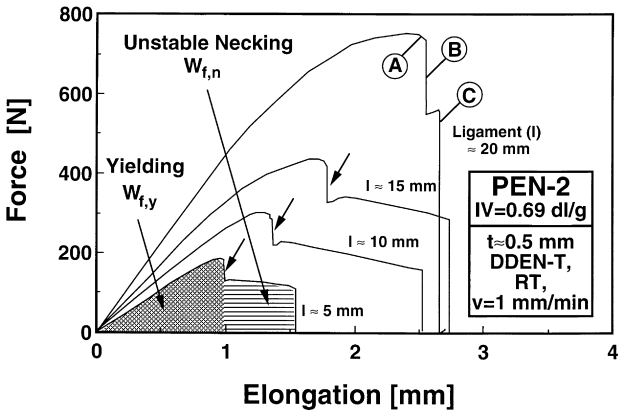

Fig. 5. Comparison of the F–x curves of DDEN-T specimens at different ligament lengths ($l \approx 5$, ≈ 10, ≈ 15 and ≈ 20 mm) for PEN-2 Note:this figure also indicates for the partition between yielding and necking.

specimens, was considered to be the limiting factor. Based on the Hill-criterion $\sigma_N \leq 1.15\sigma_y$ should hold for the DDEN-T configuration [18,21]. Fig. 7 demonstrates that even this condition was not met for all DDEN-T specimens of the PEN samples tested. If the σ_y values were determined on dumbbells having 4 mm width (type S3A according to DIN 53504) instead of 10 mm (see the reported data in Table 1), all data obeyed the Hill criterion. This suggests that the above σ_N validation should focus on the smallest allowed ligament range. Nevertheless, the conclusion from Figs. 3, 5 and 7 is that the fracture behavior of the PEN samples can only be compared if the yielding-related terms are considered (see Section 3.3)

3.3. Essential work of fracture

The appearance of the F–x curves of PENs allowed us to partition between the specific work of fracture (w_f) required for yielding ($w_{f,y}$) and that consumed by necking and fracture ($w_{f,n}$). As both $w_{f,y}$ and $w_{f,n}$ are composed terms under plane stress [9,11] Eq. (3) can be rewritten:

$$w_f = w_{f,y} + w_{f,n} = w_e + \beta w_p l \tag{7}$$

$$w_{f,y} = w_{e,y} + \beta' w_{p,y} l \tag{8}$$

$$w_{f,n} = w_{e,n} + \beta'' w_{p,n} l \tag{9}$$

Figs. 8 and 9 depict the w_f, $w_{f,y}$ and $w_{f,n}$ vs l curves for the DDENT specimens of PEN samples 4 and 2, respectively. These specific work of fracture parameters were computed from the related areas beneath the F–x curves (overall, yielding and necking, respectively, cf. Figs. 3 and 5) [9,11]. For the high MW PEN the w_f, $w_{f,y}$ and $w_{f,n}$ vs l curves showed the expected linear regressions with high correlation coefficients (see Fig. 8 and Table 2). This finding is in full agreement with similar results achieved on amorphous copolyesters [9,11]. By contrast, the linear regressions are less persuading for the PENs of low MW except the yielding related term (cf. Fig. 9 and Table 2). This was expected based on the F–x curves shown in Fig. 5 according to which both w_f and $w_{f,n}$ should experience a large scatter. The $w_{f,y}$ vs l plot, on the contrary, exhibits a high correlation coefficient (see Table 2). This substantiates our previous prediction that for a material comparison the yielding-related term is the only appropriate one. Fig. 9 shows another peculiarity: the $w_{f,n}$ vs l fit suggests a negative slope. It is obvious that this is due to the crack instability in the necking phase as discussed above. In contrast, the slope of the EWF approach can be zero but never negative. The physical meaning of the zero slope is that the specimen has ductile failure exactly in the process zone, i.e. without the formation of a plastic zone. Note that this is more or less the scenario with our PENs of low IV. As a consequence, neither w_e nor $w_{e,n}$ has any practical meaning in that case—this is the reason why these values are indicated by a question mark in Table 2. It should be mentioned here that the appearance of a negative slope in the w_f vs l indicates that some prerequisites of the EWF approach are not satisfied [3]. This is usually due to a ductile–brittle transition that takes place during loading. Recall that this was the case here, also. Mouzakis and Karger-Kocsis [22] recommended recently a simple method to overcome this difficulty and to deduce a valid $w_{e,I}$ value irrespective of a ductile–brittle transition.

The major finding with respect to the data in Table 2 is that $w_{e,y}$ is practically the same for all the PENs studied. Therefore, one can assume that the yielding performance of these PENs does not depend on the MW. Instead of MW we have to consider a structural parameter which is constant and, in addition, characterizes the amorphous glasses properly. Considering the fact that the entanglement density and thus also the M_e are constants above a threshold MW for a given thermoplastic polymer, the EWF response is likely controlled by the entanglement network. It was claimed based on the results achieved on amorphous copolyesters that $w_{e,y}$ agrees with $w_{e,I}$, i.e. with the plane strain essential work of fracture [8]. Note that $w_{e,I}$ is a material parameter per se which is related to the inherent toughness.

A further challenge is to find an easy way to estimate this material toughness parameter. Based on Fig. 7, it is obvious that such a material parameter, if any, should depend on σ_y. Hashemi [4,23] and Mai [24] have shown that:

$$w_e = \sigma_y \epsilon_{COD} \tag{10}$$

where ϵ_{COD} is the critical crack opening displacement (COD). Note that Eq. (10) was valid only for plane stress conditions. Based on the above analogy the following equation can be formulated for plane strain:

$$w_{e,I} \approx w_{e,y} = \sigma_y \epsilon_{y,0} \tag{11}$$

where $\epsilon_{y,0}$ is the DDENT specimen extension at full ligament yielding. The physical meaning of $\epsilon_{y,0}$ is the critical crack tip blunting which is completed at the instantaneous yielding. Therefore, $\epsilon_{y,0}$ is synonymous with the critical

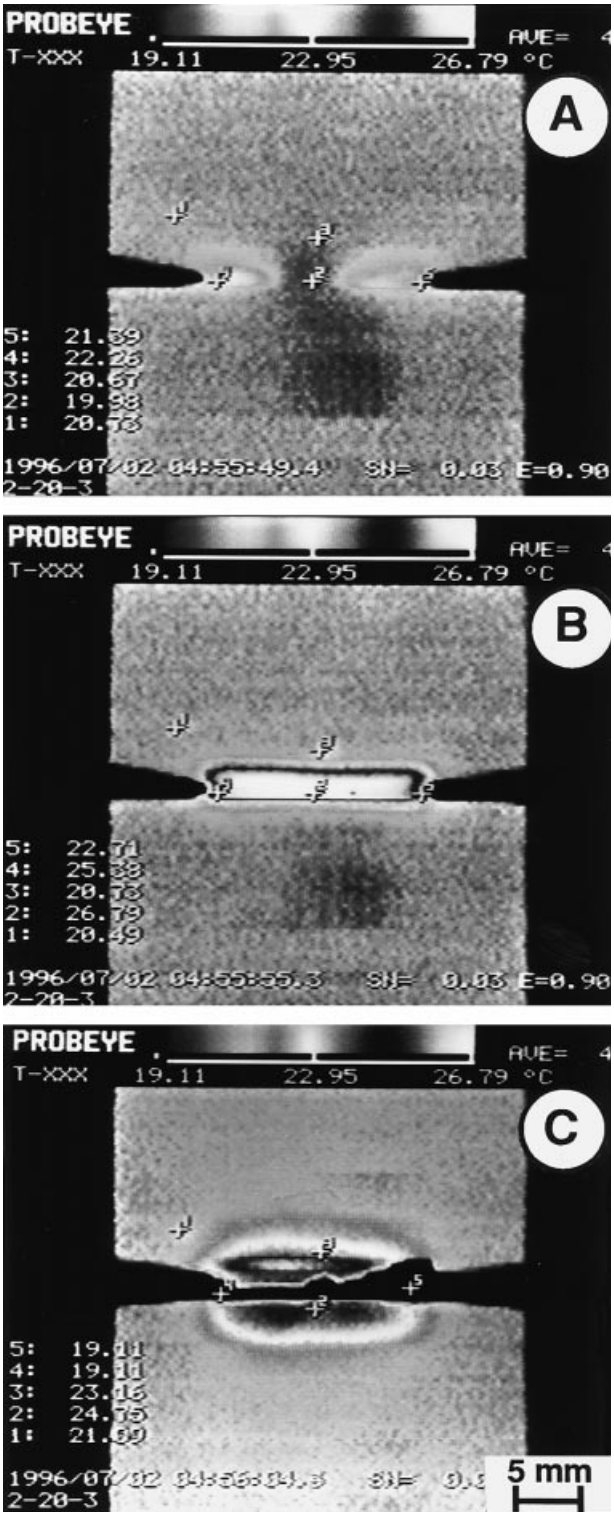

Fig. 6. Serial IRT frames taken during loading of a DDEN-T specimen of $l \approx 20$ mm of PEN-2 Note: the taking position of the IRT frames are shown in the related F–x curve in Fig. 5.

COD (i.e. at yielding). For DDEN-T specimens its value can be determined by plotting the specimen extensions at yielding as a function of the ligament (cf. Fig. 10). The extension at yielding of a DDENT-T specimen of PEN-3 is demonstrated in Fig. 11. Here the loading of the specimen was stopped just when the yielding occurred. $\epsilon_{y,0}$ is given by the linear extrapolation to $l = 0$ [4,23,24]. The $\epsilon_{y,0}$ values determined by this technique (cf. Fig. 9) are in the range of 0.35–0.41 mm (see Table 3). The $w_{e,y}$ values computed by considering Eq. (11) produced data which agreed very well with the experimental ones (cf. Table 3). The next logical question is whether or not it is possible to estimate the $\epsilon_{y,0}$ value from a load–displacement curve from a standardized dumbbell specimen. This seems to be viable for amorphous copolyesters and PEN systems where the failure starts by highly localized shear banding [7,11]. The latter can sometimes be well observed (Fig. 12) and its width is determined by suitable techniques. The underlying assumption is that the width of the shear band agrees with ϵ_{COD}, which has not yet been demonstrated. Further investigations are also needed to determine how this $\epsilon_{y,0}$ could be read from the σ–ϵ curve of the dumbbells undergoing shear banding.

Table 2
Specific essential work (w_e) and its contributing terms ($w_{e,y}$ and $w_{e,n}$) along with their correlation coefficients (R^2). Note: question marks denote unreliable data

Material	w_e (kJ/m^2)	R^2	$w_{e,y}$ (kJ/m^2)	R^2	$w_{e,n}$ (kJ/m^2)	R^2
PEN-1	61.1(?)	0.041	24.5	0.900	36.6(?)	0.245
PEN-2	67.5(?)	0.787	23.5	0.941	43.7(?)	0.212
PEN-3	43.0	0.989	22.3	0.992	20.7	0.960
PEN-4	42.2	0.977	22.4	0.980	19.8	0.970

3.4. Non-essential work of fracture

There are several options to determine the non-essential work of fracture. The direct way is to relate the work done on the plastically deformed volume of uniaxially loaded tensile dumbbell specimens [18]. Recalling that the slope of the plot of w_f vs l is equal to βw_p, the shape parameter of the plastic zone, β, can be determined. The advantage of this method is that it can be used for all the PENs studied. Its

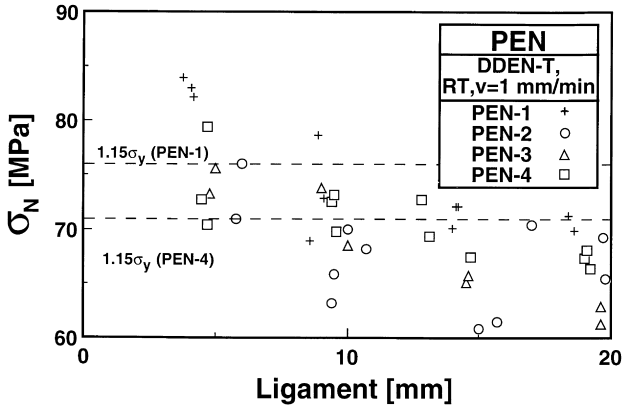

Fig. 7. σ_N vs l curves of the DDEN-T specimens of all PENs tested Note: the $1.15\sigma_y$ limit range is indicated by broken lines for PEN-1 and PEN-4.

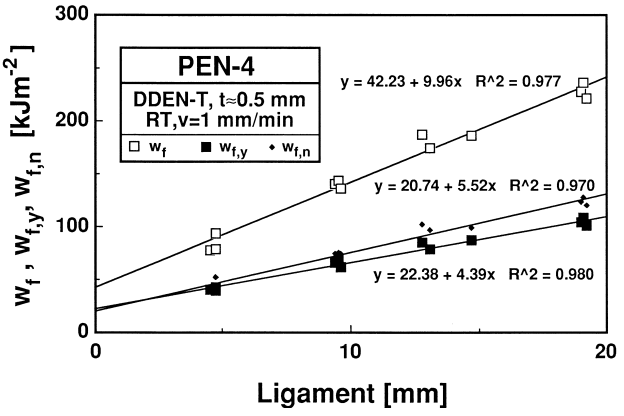

Fig. 8. Total specific work of fracture (w_f) and its contributing terms (yielding, $w_{f,y}$ and necking, $w_{f,n}$) vs ligament length (l) for the DDEN-T specimens of PEN-4.

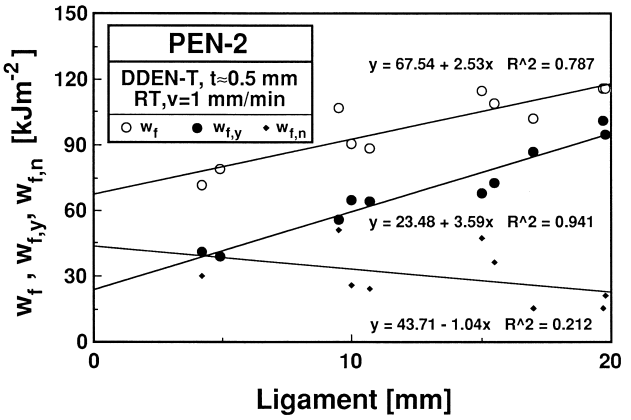

Fig. 9. Total specific work of fracture (w_f) and its contributing terms (yielding, $w_{f,y}$ and necking, $w_{f,n}$) vs ligament length (l) for the DDEN-T specimens of PEN-2.

primary disadvantage is that it relies on some uncertainty associated with assessing the deformed volume.

The indirect way is to estimate the shape parameter, β, by considering the form of the necked region. This can be done by viewing the broken specimens in light microscopy (see Section 3.5) or by evaluating the IRT heat maps taken during loading of the DDEN-T specimens (cf. Figs. 4 and 6). It should be noted that light microscopy is more reliable than the IRT, and therefore it was adopted here (Fig. 13). The shape of the plastic zone was approximated by a shallow diamond-like form for, which

$$\beta = \frac{h}{2l} \tag{12}$$

holds, where h is the overall height of the plastic zone (see Fig. 13) [18,25]. It is obvious that the indirect techniques cannot be used for PENs of low IV, i.e. for samples 1 and 2. On the contrary, the indirect estimation is suitable for the samples of high IV, i.e. No. 3 and 4. The plastic work related terms are summarized in Table 4. w_p is the subject of a great scatter range. The scatter range was substantially reduced when small width dumbbells were used. This also resulted in an increase of the "direct" w_p values which were always below the "indirect" ones. This finding corroborates our earlier observation made with respect to Fig. 7. The large difference between the "direct" and "indirect" w_p values reflects uncertainties in the determination of the deformed volume of the tensile-loaded dumbbells in the "direct" tests.

Nevertheless, based on Table 4 one can recognize that MW affects the plastic work and its terms. This note is valid also for the $\beta' w_{p,y}$ term. Recall that for plane strain where $w_{e,y} \approx w_{e,I}$, $\beta' w_{p,y}$ should be 0. By plotting $\beta' w_{p,y}$ as a function of IV and extrapolating the linear relation to $\beta' w_{p,y} = 0$ an IV = 0.2 dl/g is the outcome (Fig. 14). This may approximate the threshold MW below which no plastic deformation can take place. It is believed that this IV corresponds to the actual MW, which is related to the onset of molecular entanglement. This prediction requires, however, considerable experimental support.

The overall plastic work can likely be estimated by $\sigma_n \epsilon_b$ of the tensile experiments on dumbbells. This is based on the fact that PEN dumbbells showed practically no work hardening during the tensile test.

3.5. Failure mode

Remember that the temperature rise detected during loading of the DDEN-T specimens was less than 5°C, so that the T_g of PEN (ca. 110°C) was not reached. If it is so, the deformation of the glassy PEN polymer should have occurred via cold drawing and not by true plastic deformation. There is a simple way to check the onset of cold drawing. By keeping the broken DDEN-T specimens for a few minutes just above T_g, the plastic zone should disappear and the original shape of the DDEN-T specimen half should be restored when the deformation mode was cold drawing [9,11]. This was the case, in fact, as Fig. 15 portrays. The "shape memory" is further evidence that the initial entanglement network structure was stretched but not disrupted (except the fracture zone). The presence of a stretched entanglement network guarantees the shape recovery observed. In analogy with amorphous copolyesters [9,11] it can be argued that the mean molecular weight (M_e) between entanglements is the same for the PENs studied. This is corroborated by the IV values, which are higher than the critical one predicted for the formation of the entanglement (cf. Fig. 14). As a consequence, the high MW resins can accommodate a substantially higher network deformation than the lower MW version before final fracture. This is due to the longer molecules having more "entangling knots" and thus being able to distribute and relieve the stress in a larger volume element. It is obvious that the necking process via cold drawing is frequency (time) dependent. So, one can expect that the result of increasing deformation rate (which corresponds to a test of higher frequency) for a high MW

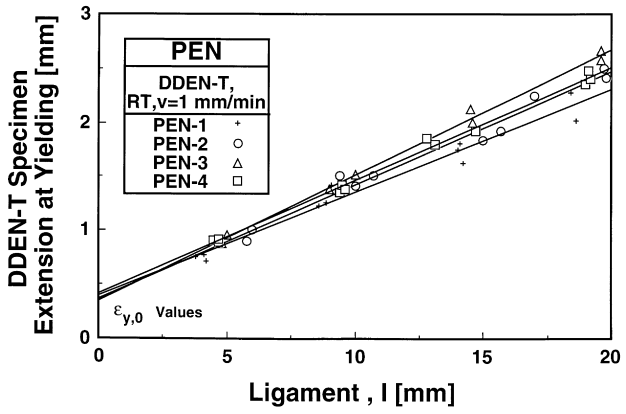

Fig. 10. Plot of the specimen extension vs ligament length for the PENs studied Note that the extrapolated $\epsilon_{y,0}$ value is practically constant.

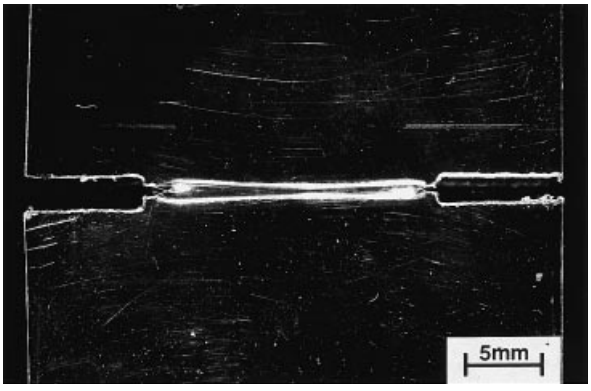

Fig. 11. Light microscopic picture taken on the yielded ligament of a DDEN-T specimen of PEN-3 with $l \approx 20$ mm.

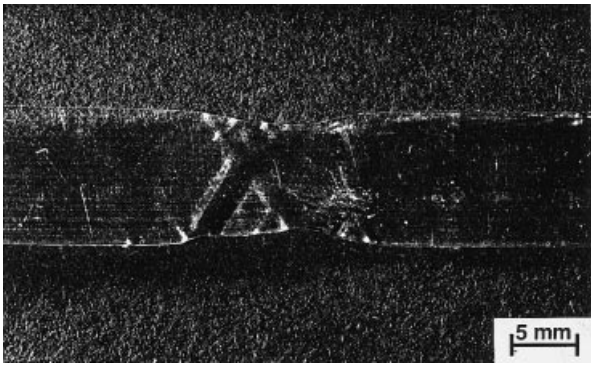

Fig. 12. Shear band formation in a dumbbell of PEN-3.

Table 3
Comparison of the experimental and calculated (Eq. (11)) $w_{e,y}$ data

Material	$w_{e,y}$ (kJ/m^2)	
	Experimental	Calculated
PEN-1	24.5	26.25
PEN-2	23.5	23.47
PEN-3	22.3	21.45
PEN-4	22.4	25.02

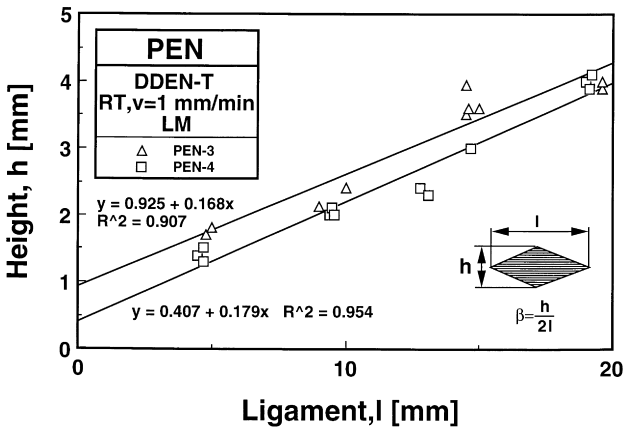

Fig. 13. Total height of the plastic zone (h) determined by light microscopy as a function of the ligament length (l) for DDEN-T specimens of PEN-3 and PEN-4.

resin should bring similar results as samples of low MW resin tested at a lower deformation rate. Preliminary results performed on PEN-3 in the range of $v = 1$–100 mm/min seems to confirm this expectation [26].

The broken halves of a DDEN-T specimen of a low MW PEN is shown in Fig. 16. One can recognize a more confined "plastic" zone compared to the high MW resins (cf. Fig. 15). Furthermore, the fracture path of the specimen resembles saw teeth, the appearance of which is a clear indication for insufficient stress transfer via the entangled molecules of shorter length. When the network deformability is exhausted in a low MW PEN, then microcracking takes place. The run of the microcracks, which are inclined to the process zone near to 45°, indicates that the network deformation was shear-dominated. The effect of cold drawing should be manifested in strain-induced crystallization that was shown for amorphous copolyesters [19] and found also for these PEN samples.

4. Conclusions

The plane stress ductile fracture behavior of amorphous PEN films of varying molecular weights (MW) was studied by the essential work of fracture (EWF) method using deeply double-edge notched tensile (DDEN-T) specimens. The MW of the PEN samples was characterized by the intrinsic solution viscosity (IV). Based on this study the following conclusions may be drawn:

1. The EWF works well for PENs because they undergo full ligament yielding prior to the onset of crack growth. Based on the indication of yielding in the load–displacement curve, it was possible to partition between the specific essential and non-essential parts of work of fracture required for yielding ($w_{e,y}$ and $w_{p,y}$) and for subsequent necking ($w_{e,n}$ and $w_{p,n}$). MW did not influence $w_{e,y}$, which was suggested to be a real material parameter. It was argued that the EWF response of PEN is governed by

Table 4
Parameters of the non-essential or plastic work (w_p) determined by direct and indirect (light microscopic, LM) methods. Note: the direct w_p values show the scatter range of five parallel tests

Material	Direct method		Indirect method		
	Dumbbell: Type 3 w_p (MJ/m^3)	Type S3A w_p (MJ/m^3)	βw_p(MJ/m^3)	β_{LM}	w_p(MJ/m^3)
PEN-1	55–66	68–74	–	–	–
PEN-2	60–71	72–79	–	–	–
PEN-3	76–83	89–95	8.79	0.084	104.6
PEN-4	78–86	90–93	9.96	0.090	110.7

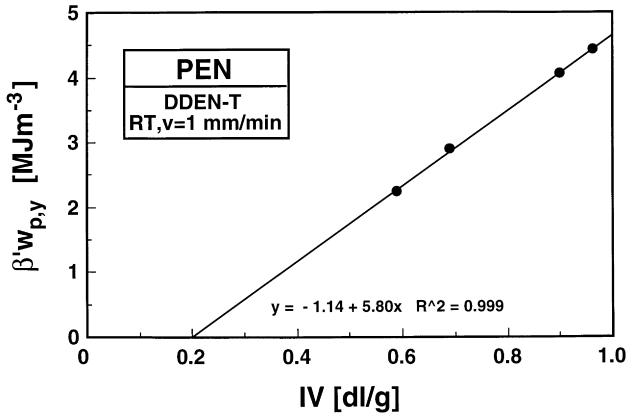

Fig. 14. Plot of $\beta' w_{p,y}$ vs IV for all PENs studied.

the entanglement network density. The $w_{e,y}$ could be well estimated by the term $\sigma_y \epsilon_{y,0}$, where σ_y is the yield stress and $\epsilon_{y,0}$ is the crack opening displacement at yielding.

2. MW affected the postyielding (necking) behavior. Necking occurred by cold drawing and not by true plastic deformation. This was shown by the shape recovery of the specimen for which a stretched but not disrupted entanglement network was believed to be responsible. The difference in the failure mode between low (unstable crack growth) and high MW (stable crack growth) PEN resins was traced to the load distribution capacity of the longer entangled molecules. It was predicted that the network deformation is frequency-dependent and a high frequency test on a high MW resin should correspond to the low frequency test on a low MW PEN.

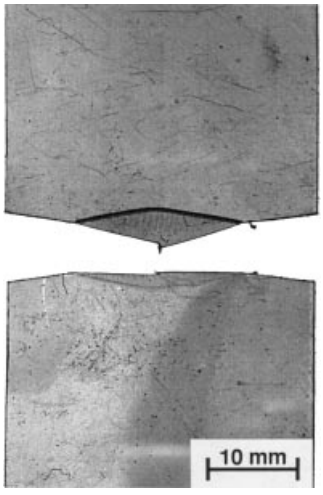

Fig. 15. Macrophotograph of the ligament area of a failed DDEN-T specimen of PEN-3 before (top) and after annealing (bottom) just above the T_g.

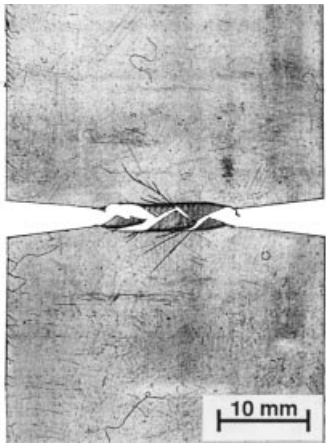

Fig. 16. Macrophotograph of the ligament area of a failed DDEN-T specimen of PEN-2.

Acknowledgements

The authors thank Dr T. Czigány (TU Budapest) for his help in performing the EWF tests and to the Eastman Chemical Co. for the release of this paper.

References

[1] Broberg KB. J Mech Phys Solids 1971;19:407.
[2] Broberg KB. J Mech Phys Solids 1975;23:215.
[3] Mai Y-W, Wong S-C, Chen X-H. Application of fracture mechanics for determination of toughness of polymer blends (chap. 20). In: Paul DR, Bucknall CB, editors. Polymer blends: formulations and performance, New York: Wiley, 1999;2:17–58.
[4] Hashemi S. J Mater Sci 1997;32:1563.
[5] Hashemi S. Plast Rubber Compos Process Appl 1993;20:229.
[6] Ferrer-Balas D, Maspoch ML, Martinez AB, Santana OO. Polym Bull 1999;42:101.
[7] Karger-Kocsis J. Polym Bull 1996;27:119.

[8] Karger-Kocsis J, Czigány T, Moskala EJ. Polymer 1997;38:4587.
[9] Karger-Kocsis J, Czigány T, Moskala EJ. Polymer 1998;39:3939.
[10] Karger-Kocsis J, Czigány T, Moskala EJ. Polym Engng Sci 1999;39:1404.
[11] Karger-Kocsis J, Moskala EJ. Polym Bull 1997;39:503.
[12] Hashemi S. Polym Engng Sci 1997;37:912.
[13] Karger-Kocsis J. Macromol Symp 1999;143:185.
[14] Karger-Kocsis J. Fracture and fatigue behavior of semicrystalline polymers as a function of microstructural and molecular parameters in structure development. In: Cunha AM, Fakirov S, editors. Processing for Polymer Property Enhancement NATO-ASI, Dordrecht: Kluwer, 2000 (in press).
[15] Brown HR. Macromolecules 1991;24:2752.
[16] Wu S. Polym Engng Sci 1990;30:753.
[17] Hui CY, Kramer EJ. Polym Engng Sci 1995;35:419.
[18] Testing Protocol for Essential Work of Fracture, ESIS TC-4 Group, 1993.
[19] Karger-Kocsis J, Shang PP, Moskala EJ. J Therm Anal Calorimetry 1999;55:21.
[20] Cañadas JC, Diego JA, Mudarra M, Belana J, Díaz-Calleja R, Sanchis MJ, Jaimés C. Polymer 1999;40:1181.
[21] Hill H. J Mech Phys Solids 1952;4:19.
[22] Mouzakis DE, Karger-Kocsis J. Polym Bull 1999;42:473.
[23] Paton CA, Hashemi S. J Mater Sci 1992;27:2279.
[24] Seth RS, Robertson AG, Mai Y-W, Hoffmann JD. Tappi J 1993;76:109–16.
[25] Atkinson AG, Mai Y-W. Elastic and plastic fracture, Chichester: Ellis Horwood, 1988. p. 298–312.
[26] Karger-Kocsis J, Czigány T. Polym Engng Sci 2000 (in press).